POLITECNICO DI TORINO
Repository ISTITUZIONALE

Nonlinear response of magnetic islands to localized electron cyclotron current injection

Publisher copyright

(Article begins on next page)

04 August 2020

Nonlinear response of magnetic islands to localized electron cyclotron current injection

D. Borgogno, L. Comisso, D. Grasso, and E. Lazzaro

Articles you may be interested in

Nonlinear evolution of three-dimensional instabilities of thin and thick electron scale current sheets: Plasmoid formation and current filamentation
Phys. Plasmas **21**, 072306 (2014); 10.1063/1.4887279

Three dimensional instabilities of an electron scale current sheet in collisionless magnetic reconnection
Phys. Plasmas **21**, 062116 (2014); 10.1063/1.4885636

Kelvin-Helmholtz instability in a current-vortex sheet at a 3D magnetic null
Phys. Plasmas **20**, 032117 (2013); 10.1063/1.4798516

Nonlinear stability of magnetic islands in a rotating helical plasma
Phys. Plasmas **19**, 122510 (2012); 10.1063/1.4773041

Nonlinear response of a neoclassical four-field magnetic reconnection model to localized current drive
Phys. Plasmas **17**, 052509 (2010); 10.1063/1.3428676

Nonlinear response of magnetic islands to localized electron cyclotron current injection

D. Borgogno,[1,2] L. Comisso,[2,3] D. Grasso,[2,3] and E. Lazzaro[4]
[1]Dipartimento di Fisica, Università di Pisa, Pisa, Italy
[2]Dipartimento Energia, Politecnico di Torino, Torino, Italy
[3]Istituto Sistemi Complessi—CNR, Roma, Italy
[4]Istituto di Fisica del Plasma "P.Caldirola," Associazione Euratom-ENEA-CNR, Milano, Italy

The magnetic island evolution under the action of a current generated externally by electron cyclotron wave beams is studied using a reduced resistive magnetohydrodynamics plasma model. The use of a two-dimensional reconnection model shows novel features of the actual nonlinear evolution as compared to the zero-dimensional model of the generalized Rutherford equation. When the radio frequency control is applied to a small magnetic island, the complete annihilation of the island width is followed by a spatial phase shift of the island, referred as "flip" instability. On the other hand, a current-drive injection in a large nonlinear island can be accompanied by the occurrence of a Kelvin-Helmholtz instability. These effects need to be taken into account in designing tearing mode control systems based on radio frequency current-drive. © 2014 AIP Publishing LLC.
[http://dx.doi.org/10.1063/1.4885635]

The tearing modes, generated by a reconnection process, are a serious cause of degradation of plasma confinement in the Tokamak devices. An important open issue is to find appropriate means for the control of such instabilities. One of the most promising methods suitable to counteract robustly the tearing instabilities in a Tokamak is based on the injection of an external control current within the magnetic island.[1–3] The electron cyclotron current-drive (ECCD) is very appropriate for this purpose, due to its localized deposition.[4] The driven current can both modify locally the equilibrium[5] and counteract the unstable perturbation which evolves into a magnetic island.[6] Experimental results have demonstrated successful stabilization on several devices.[2,3,7–10]

The conventional approach on which practical control systems are being designed is based on the zero-dimensional (0-D) model of the (generalized) Rutherford equation[1,2,6] describing the time evolution of the nominal width of the island. Although largely applied, in this approach the fundamental topological aspects of the problem are hidden, as pointed out in Refs. 11 and 13–15.

With the aim of going beyond this 0-D description, in this paper we isolate and discuss basic aspects of the problem of control of magnetic reconnection adopting the simplest nonlinear reduced magnetohydrodynamics (MHD) model with the addition of a radio frequency driven current. In particular, we present new results concerning the effect of ECCD on the dynamics of tearing modes, which depends on the power and width of the beam as well as on the magnetic island width. In order to analyze the effect on magnetic islands of different sizes, the control current is turned on during the linear, the nonlinear, and the saturated phases of an unstable reconnection process. A continuously driven control current has been adopted, peaked at a fixed point of the evolving magnetic island.

A two-dimensional (2-D) slab description based on the standard Reduced Resistive MHD Model (RRMHD)[16] has been used. The contribution of the externally imposed ECCD is represented by a source term J_{ec} in the plasma Ohm's law. The evolution equation of the poloidal magnetic flux function ψ and the vorticity U is

$$\frac{\partial \psi}{\partial t} + \mathbf{v}_\perp \cdot \nabla \psi = -\eta(J - J^{(0)} - J_{ec}), \quad (1)$$

$$\frac{\partial U}{\partial t} + \mathbf{v}_\perp \cdot \nabla U = \mathbf{B}_\perp \cdot \nabla J. \quad (2)$$

The total magnetic field is $\mathbf{B} = B_0 \mathbf{e}_z + \mathbf{B}_\perp$, the in-plane magnetic field is $\mathbf{B}_\perp = \nabla \psi \times \mathbf{e}_z$, the in-plane velocity is $\mathbf{v}_\perp = -\nabla \varphi \times \mathbf{e}_z$, and $U = \mathbf{e}_z \cdot (\nabla \times \mathbf{v}_\perp) = \nabla_\perp^2 \varphi$, where φ is the stream function. The current density is $J = \mathbf{e}_z \cdot (\nabla \times \mathbf{B}_\perp) = -\nabla_\perp^2 \psi$, $J^{(0)}$ is its equilibrium component, and η is the plasma resistivity. All lengths are scaled to the macroscopic equilibrium magnetic field scale length L, while the time is normalized on the Alfvèn time τ_A, defined by the equilibrium poloidal magnetic field. The profile of the control current-density is assumed to be Gaussian and distributed uniformly on the magnetic surfaces $\psi = const$.

$$J_{ec}(x,y,t) = J_m(t)\exp\left(-\frac{(\psi(x,y,t) - \psi_O(t))^2}{\delta^2}\right), \quad (3)$$

where ψ_O is the magnetic flux as a function of time, evaluated at the original island O-point. This is a general representation for non-inductively driven current.[12] In order to single out the space scale effects of the radio frequency driven current, we have deliberately assumed that all the energy input associated with the current-drive process (EC waves heating) is balanced by heat losses. The aim of a control current like Eq. (3) is to restore the ideal frozen flux condition in Eq. (1), by reducing the perturbed current density $J - J^{(0)}$. This is expected to counterbalance the unstable

reconnection process and eventually to stop the magnetic island growth.[13,17,18] The peak amplitude J_m has a step function time waveform

$$J_m(t) = \begin{cases} 0 & t < t_1 \;\; \vee \;\; t > t_2 \\ A & t_1 < t < t_2, \end{cases} \qquad (4)$$

where t_1 and t_2 are the switching on and switching off time of the current control, respectively. The amplitude A is a constant, $A = -a \cdot (J_X(t_1) - J_O(t_1))$, and the width δ is evaluated in the ψ space as $\delta = b \cdot (\psi_X(t_1) - \psi_O(t_1))$, where X and O subscripts denote the $X-$ and $O-$point positions at $t = t_1$, respectively.

Equations (1) and (2) are integrated numerically by the code used in Ref. 19. We set up a numerical experiment of spontaneous magnetic reconnection process in a static, "Harris pinch" equilibrium configuration with $B_{\perp y}^{(0)} = B_y^{(0)} \tanh(x/L)$ and $\mathbf{v}_{\perp}^{(0)} = 0$, where $B_y^{(0)} = 1$ and $L = 1$. This equilibrium is tearing mode unstable if the instability parameter Δ' $= 2 \cdot (1/k_y - k_y) > 0$, where $k_y = 2\pi m/L_y$, being m the corresponding mode number and L_y the length of the domain along the y-direction. The box extension along the x direction is $L_x = 22.64$, which avoids any influence of boundary conditions on the reconnection dynamics. We perturb the equilibrium configuration with a current-density disturbance and assume a plasma resistivity $\eta = 5 \times 10^{-4}$. A mesh of $nx = ny = 1024$ grid points has been adopted. In the following, we present figures relative to cases with $L_y = 8\pi$, which corresponds to $(\Delta', m) = \{(7.5, 1), (3, 2), (1.167, 3)\}$ for the only three unstable modes. This equilibrium configuration justifies our choice of neglecting the polarization current effects in Eq. (2). Its stabilizing contribution, in fact, is expected to be relevant only for weakly unstable modes ($\Delta' \ll 1$). The time evolution of the reconnection process is monitored through the variation of the area $A_{isl}(t)$ enclosed by the separatrix of the magnetic island. This choice finds its justification in that the control current can strongly deform the magnetic island in such a way that the Rutherford island width is no longer a reliable quantity.

The effect of application of ECCD control is studied for three different island sizes corresponding to different stages of the free reconnection process, i.e., without control current, whose evolution is shown in Fig. 1. Simulations have been carried out by scanning the J_{ec} parameters in the intervals $1 \leq |J_m/(J_X - J_O)|_{t_1}| \leq 10$ and $0.1 \leq \delta/(\psi_X - \psi_O)|_{t_1} \leq 1$.

The ECCD injection for small islands, corresponding to the linear and early nonlinear regimes ($w \ll L$), is analyzed through the results of the simulations reported in Fig. 2. All the curves exhibit the same initial behavior: after the island suppression around $t \approx 430$, the area of the island bounces back with a growth rate equal to the previous rate of quench. In other words, the effect of the applied current meant to restore the stability of small islands (so called "early" control action) may lead, on the contrary, to another unstable state. This is a state bifurcation that, in the context of reconnection driven by boundary perturbations, is known as *flip* instability[20,21] because the value of the reconnected flux $\psi_X - \psi_O$ changes sign. This is equivalent to a shift of $L_y/2$ of the equilibrium position of the elliptic O-point of the tearing
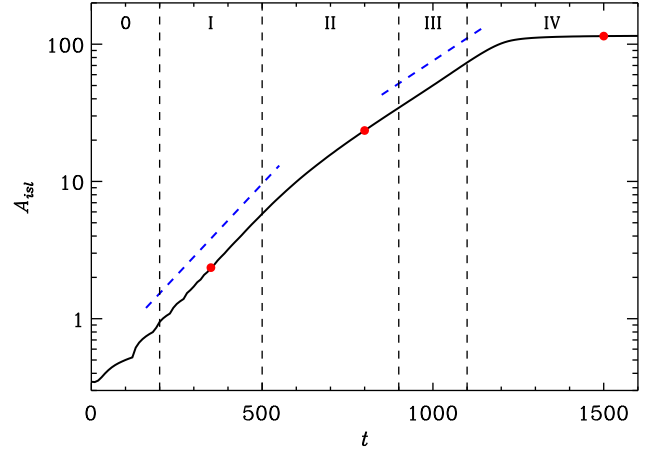

FIG. 1. Magnetic island area vs time for the free evolving system: 0-initial transient, I-linear exponential growth, II-algebraic regime, III-second exponential phase, and IV-saturation. The bullets indicate the instants at which the current drive has been switched on.

perturbation. It is noteworthy that this behavior is found here, with universal characteristics, in the frame of the so-called non-inductive current-drive effects where it has been always ignored. After the first flip, the magnetic island grows monotonically for the lowest b parameter, while, for the other two cases, it reaches a maximum after which a new decreasing phase follows until a second flip occurs. We have verified that this flip instability is independent from the value of the equilibrium Δ'.

To understand the mechanism of the ECCD control on thin magnetic islands, we evaluate Eq. (1) at the X- and O-points of the island and subtract them obtaining

$$\frac{\partial(\psi_X - \psi_O)}{\partial t} = -\eta(J_X - J_O - J_{ecX} + J_{ecO}). \qquad (5)$$

In the small island width approximation, $w \ll L$, $w^2 = -8(\psi_X - \psi_O)/J^{(0)}(0)$, our equilibrium and current-drive choices lead to the following equation:

$$\frac{\partial w^2}{\partial t} = 8\eta(J_X - J_O \mp J_m(e^{\frac{-w^4}{8\delta^2}} - 1)), \qquad (6)$$
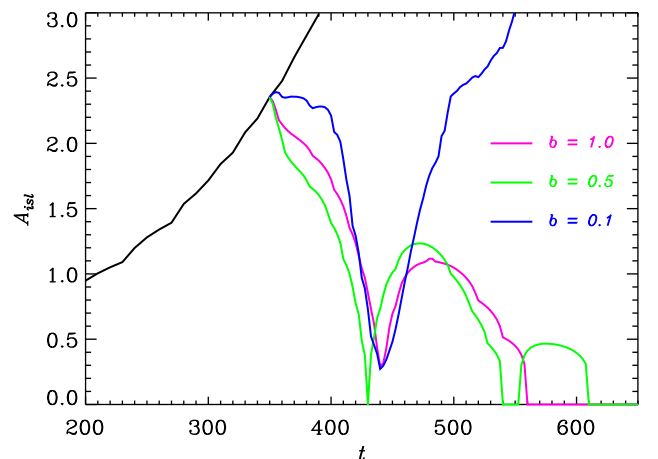

FIG. 2. Time evolution of the magnetic island area for three different values of the normalized current-drive width $b = \delta/(\psi_X - \psi_O)|_{t_1}$. The ECCD has been switched on at $t_1 = 350$ with a maximum height of $|J_m| = 10 \cdot (J_X - J_O)|_{t_1}$.
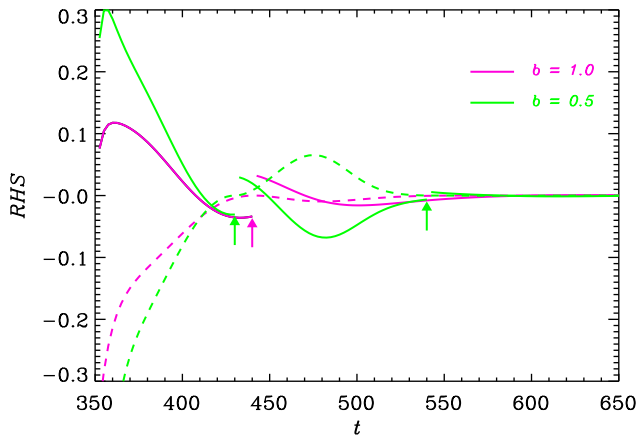
FIG. 3. Time evolution of the RHS of Eq. (5) for the cases $b = \delta/(\psi_X -\psi_O)|_{t_1} = 1$ and $b = 0.5$. Solid lines correspond to the $J_X - J_O$ term, while dashed lines show the $J_{ecO} - J_{ecX}$ term. The discontinuities, shown by the arrows, are due to the island *flip*, when the $X-$ and the $O-$points suddenly shift of $L_y/2$.

FIG. 4. Time evolution of the controlled magnetic island area for ECCD currents with different peak amplitudes J_m and a fixed beam width $\delta = 0.5 \cdot (\psi_X - \psi_O)|_{t_1}$. The control current injection starts at $t_1 = 800$.

where the minus occurs when J_{ec} peaks on the O-point and the plus when it peaks on the X-point. Equation (6) reveals that the growth of the magnetic island depends on the balance of the total current $(J - J_{ec})$ between the X- and O-points of the island. Note that the nonlinearity of this behavior is hidden in the fact that the plasma current density, J, depends strongly on the injected current, J_{ec}. The ECCD contribution to the island evolution equation becomes negligible at the flip because of the island suppression. Since the equilibrium configuration is still unstable, the magnetic island starts to grow again, driven by the positive sign of the dominant term in the RHS of Eq. (5) right after the flip, $J_X - J_O$. In the two cases with higher b parameter, the growth ends around $t = 460$, when, the ECCD contribution is likely to restore the negative sign of the RHS, as shown in Fig. 3. From now on the island shrinks again until $t = 540$. It is remarkable that this happens even though the ECCD is centered at the island X-point after the flip. This is because in presence of a wide ECCD beam a significant amount of the control current reaches the region around the island O-point, which is the optimal deposition site. The case $\delta = 0.1$ behaves differently because the injected current is strongly located at the X-point, driving new unstable modes that lead to a strong modification of the magnetic island and to a total loss of the control.

For larger islands, the effect of J_{ec} is investigated by turning on the control current at $t_1 = 800$, when the magnetic island has reached a macroscopic size $w \approx 1.6$. In this phase, we never observed the complete suppression of the deformation of the magnetic topology. The evolution of the area of the magnetic island for different values of J_m and a fixed $\delta = 0.5 \cdot (\psi_X - \psi_O)|_{t_1}$ is shown in Fig. 4. Low values of the peak amplitude J_m, i.e., $a = |J_m/(J_X - J_O)|_{t_1}| \leq 2$, have proven rather ineffective in counteracting the main $m = 1$ component of the magnetic flux function perturbation. The magnetic island area reduces almost monotonically on much longer time scales than those observed in controlling small islands. A faster island contraction is observed when $a = |J_m/(J_X - J_O)|_{t_1}| \geq 3$. In this case, however, the nonlinear growth of higher order
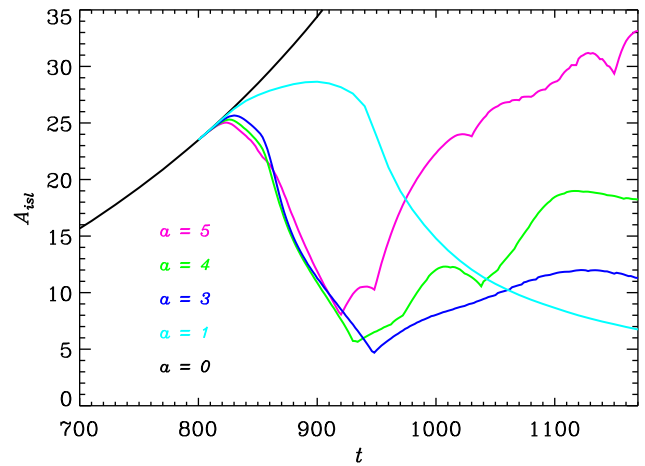
harmonics of the magnetic perturbation prevents the island suppression. This is due to the onset of a secondary Kelvin-Helmholtz (KH) instability[22] which affects the strong sheared plasma flows that form at the initial stages of the control process. The island response to the ECCD injection leads to thin, bar shaped, velocity layers similar to jets distributed along the $x = \pm x_{KH}$ axes in Fig. 5 (top panel). The plasma velocity inside the jets strongly depends on the width of the ECCD beam, while it is almost insensitive to its amplitude. In particular, smaller values of the width lead to higher shear flows. The maximum jet velocity we observed is of order $V_A/10$, where $V_A = L/\tau_A$. The magnetic field at x_{KH} has a dominant B_y component, that is significantly reduced compared to the initial equilibrium value. Hence, the stabilizing effect of the magnetic field on the plasma jets is weak and the KH instability can develop. For large ECCD beam, the jets are broadened (Fig. 5, central panel), while they are almost completely disrupted for smaller widths (Fig. 5, bottom panel). The KH instability affects not only the velocity and vorticity patterns but also responsible for the distortion of the magnetic island separatrices. The magnetic surfaces $\psi = const.$ are in fact advected by the plasma velocity towards the resonant surface $x = 0$ where they are forced to reconnect. This results in the formation of secondary island chains, corresponding to a wide spectrum of modes for the magnetic flux field, with multiple $X-$ and $O-$points, whose position and number vary in time. Such complex topology interferes with the ECCD control action. In fact, after an initial decrease, the evolution of the magnetic island area exhibits a new growth when these secondary modes in the ψ spectrum become comparable to the originally dominant $m = 1$ component. It is worth noting that while the onset of the KH instability depends also on the particular value of Δ' we are considering, the phenomenon of the bars formation on each side of the resonant surface is quite general, as we recover it also for lower values of Δ'.

The ECCD effect on a magnetic island in the saturation regime has been analyzed by turning on the control current at the time $t = 1500$ of the free system evolution, characterized by a very large island size. In this case, the magnetic island never shrinks to zero. This is true also for the less
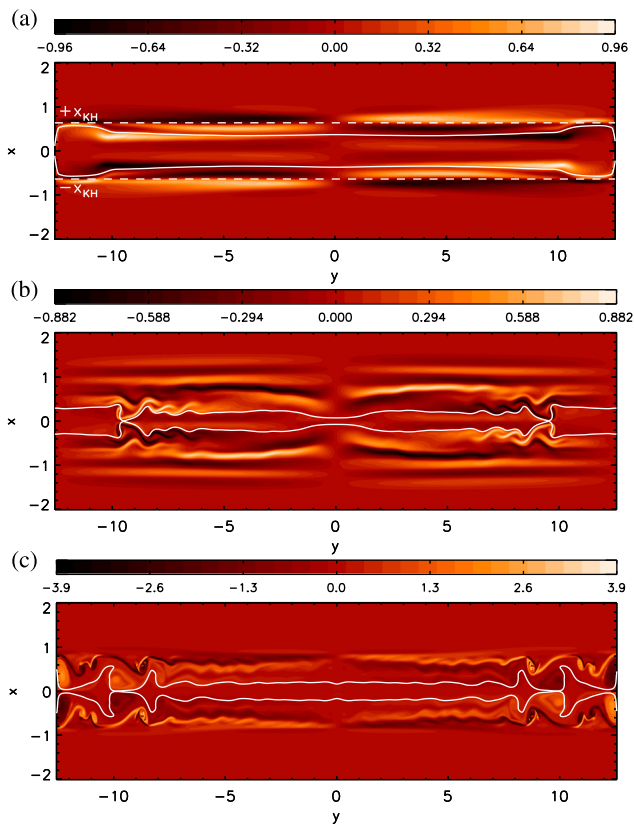
FIG. 5. Contour plots of the vorticity field and the corresponding magnetic island separatrices (white lines). Top and central panels correspond to the case shown in purple in Fig. 4 with $a = 5$, $b = 0.5$ at two different times: $t = 866$ and $t = 942$, respectively. Bottom panel corresponds to a case with $a = 5$, $b = 0.1$ at $t = 878$, corresponding to an island area comparable to the one shown in the previous frame.

unstable equilibrium configuration $(\Delta', m) = \{(1.667, 1), (-1.167, 2), (-3, 3)\}$ for which we performed the numerical simulations. Instead, as also shown in some recent works,[13,14,23] the ECCD injection into a macroscopic island leads to a new equilibrium configuration with two thin current sheets that are symmetrically localized on both sides of the resonant surface $x_s = 0$ and a macroscopic deformation of the magnetic topology (not shown here). These current layers bound the region where J_{ec} is distributed and enclose the part of the domain where the perturbed fields are different from zero.

In this work, we have studied, in the framework of a 2-D analysis, the effect of the ECCD control on a magnetic island during its entire life: from the birth, all the way through the growth to saturation. For small islands, we find that their complete suppression is followed by a new growth due to the occurrence of a *flip* instability. A similar phase instability has long been known in the context of the control of magnetic islands with external resonant magnetic perturbations.[20,21,24,25] Here, for the first time, we show why, from essential physics and mathematics, the same occurs in the case of ECCD control; we believe our arguments can help interpreting and understanding the failed attempts of ECCD control, alongside with the successful ones.

When the ECCD control is applied to a large size island, the dynamics of the magnetic island evolution is characterized

by the appearance of secondary harmonics and by the modification of the original magnetic equilibrium. This highly nonlinear behavior leads to the onset of a KH instability when the EC wave beam width is much smaller than the island size, reducing the control action, which is designed specifically for decreasing the primary, most unstable harmonic.

When we consider large saturated island it becomes more difficult to suppress the island. We may conjecture that this is due to the fact that the equilibrium configuration of the saturated state is a stable one. For this reason, we believe it is important to focus on an early control action on small magnetic islands, as also suggested in Ref. 11.

The ECCD control models of tearing modes based on the conventional 0-D Rutherford equation present very stringent requirements on the focusing of the EC wave beam on the magnetic island. Here, we have shown that, including finite 2-D nonlinear effects, a successful control action requires broader current injection. However, this may turn in a rapid drop of the control efficiency, since a relevant fraction of the injected current falls outside the separatrices, even in presence of small magnetic island reduction.

In spite of the rudimentary character of the RRMHD model we adopted, our results are quite general and remain valid also for the control of magnetic islands formed through neoclassical effects. We expect as well that the inclusion of the diamagnetic effects does not affect our results. The contribution of the island rotation has been taken into account in our analysis by fixing the ECCD control to the O-point of the magnetic island.

[1]H. Zohm, Phys. Plasmas **4**, 3433 (1997).
[2]R. J. La Haye, Phys. Plasmas **13**, 055501 (2006).
[3]I. T. Chapman, R. J. La Haye, R. J. Buttery, W. W. Heidbrink, G. L. Jackson, C. M. Muscatello, C. C. Petty, R. I. Pinsker, B. J. Tobias, and F. Turco, Nucl. Fusion **52**, 063006 (2012).
[4]J. Fisch, Rev. Mod. Phys. **59**, 175 (1987).
[5]A. Pletzer and F. W. Perkins, Phys. Plasmas **6**, 1589 (1999).
[6]C. Hegna and J. D. Callen, Phys. Plasmas **4**, 2940 (1997).
[7]G. Gantenbein, H. Zohm, G. Giruzzi, S. Günter, F. Leuterer, M. Maraschek, J. Meskat, Q. Yu, ASDEX Upgrade Team, and ECRH-Group (AUG), Phys. Rev. Lett. **85**, 1242 (2000).
[8]M. Maraschek, G. Gantenbein, Q. Yu, H. Zohm, S. Günter, F. Leuterer, A. Manini, ECRH Group, and ASDEX Upgrade Team, Phys. Rev. Lett. **98**, 025005 (2007).
[9]F. A. G. Volpe, M. E. Austin, R. J. La Haye, J. Lohr, R. Prater, E. J. Strait, and A. S. Welander, Phys. Plasmas **16**, 102502 (2009).
[10]T. P. Goodman, F. Felici, O. Sauter, J. P. Graves, and TCV Team, Phys. Rev. Lett. **106**, 245002 (2011).
[11]Q. Yu, D. Zhang, and S. Gunter, Phys. Plasmas **11**, 1960 (2004).
[12]A. H. Reiman, Phys. Fluids **26**, 1338 (1983).
[13]L. Comisso and E. Lazzaro, Nucl. Fusion **50**, 125002 (2010).
[14]E. Lazzaro and L. Comisso, Plasma Phys. Controlled Fusion **53**, 054012 (2011).
[15]A. Poyé, O. Agullo, A. Smolyakov, S. Benkadda, and X. Garbet, Phys. Plasmas **20**, 020702 (2013).
[16]H. R. Strauss, Phys. Fluids **19**, 134 (1976).

[17]R. Prater, Phys. Plasmas **11**, 2349 (2004).

[18]J. Woodby, E. Schuster, G. Bateman, and A. H. Kritz, Phys. Plasmas **15**, 092504 (2008).

[19]D. Grasso, D. Borgogno, and F. Pegoraro, Phys. Plasmas **14**, 055703 (2007).

[20]D. A. Monticello, R. B. White, and M. N. Rosenbluth, in *Proceedings of the 7th IAEA International Conference, Tokyo*, Paper No. IAEA-CN-37/K-3 (Plasma Phys. Controlled Nucl. Fusion Res., 1978) Vol. 1, p. 605.

[21]E. Lazzaro and R. Coelho, Eur. Phys. J. D **19**, 97 (2002).

[22]S. Chandrasekhar, *Hydrodynamic and Hydromagnetic Stability* (Oxford University Press, 1961).

[23]E. Lazzaro, L. Comisso, and L. Valdettaro, Phys. Plasmas **17**, 052509 (2010).

[24]A. W. Morris, T. C. Hender, J. Hugill, P. S. Haynes, P. C. Johnson, B. Lloyd, D. C. Robinson, C. Silvester, S. Arshad, and G. M. Fishpool, Phys. Rev. Lett. **64**, 1254 (1990).

[25]D. L. Nadle, C. Cates, H. Dahi, M. E. Mauel, D. A. Maurer, S. Mukherjee, G. A. Navratil, M. Shilov, and E. D. Taylor, Nucl. Fusion **40**, 1791 (2000).